Electronic phenomena at complex oxide interfaces: insights from first principles

2010 J. Phys.: Condens. Matter 22 043001

(http://iopscience.iop.org/0953-8984/22/4/043001)

J. Phys.: Condens. Matter **22** (2010) 043001 (14pp) doi:10.1088/0953-8984/22/4/043001

TOPICAL REVIEW

Electronic phenomena at complex oxide interfaces: insights from first principles

Rossitza Pentcheva[1] **and Warren E Pickett**[2]

[1] Department of Earth and Environmental Sciences, University of Munich, Theresienstrasse 41, D-80333 Munich, Germany
[2] Department of Physics, University of California Davis, Davis, CA 95616, USA

Received 2 November 2009
Published 12 January 2010
Online at stacks.iop.org/JPhysCM/22/043001

Abstract

Oxide interfaces have attracted considerable attention in recent years due to the emerging novel behavior which does not exist in the corresponding bulk parent compounds. This opens possibilities for future applications in oxide-based electronics and spintronics devices. Among the different materials combinations, heterostructures containing the two simple band insulators $LaAlO_3$ and $SrTiO_3$ have advanced to a model system exhibiting unanticipated properties ranging from conductivity, to magnetism, even to superconductivity. Electronic structure calculations have contributed significantly towards understanding these phenomena and we review here the progress achieved in the past few years, also showing some future directions and perspectives. A central issue in understanding the novel behavior in these oxide heterostructures is to discover the way (or ways) that these heterostructures deal with the polar discontinuity at the interface. Despite analogies to polar semiconductor interfaces, transition metal oxides offer much richer possibilities to compensate the valence mismatch, including, for example, an electronic reconstruction. Moreover, electronic correlations can lead to additional complex behavior like charge disproportionation and order, magnetism and orbital order. We discuss in some detail the role of finite size effects in ultrathin polar films on a nonpolar substrate leading to another intriguing feature—the thickness-dependent insulator-to-metal transition in thin $LaAlO_3$ films on a $SrTiO_3(001)$ substrate, driven by the impending polar catastrophe. The strong and uniform lattice polarization that emerges as a response to the potential build-up enables the system to remain insulating up to a few layers. However, beyond a critical thickness there is a crossover from an ionic relaxation to an electronic reconstruction. At this point two bands of electron and hole character, separated both in real and in reciprocal space, have been shifted sufficiently by the internal field in $LaAlO_3$ to impose the closing of the bandgap. We discuss briefly further parameters that allow one to manipulate this behavior, e.g. via vacancies, adsorbates or an oxide capping layer.

(Some figures in this article are in colour only in the electronic version)

Contents

1. Introduction to polar oxide surfaces and interfaces

As common as ionic insulators are—your table salt, for example—electronically they are very specific materials. In the band picture of electronic structure, in a conventional (band) insulator the Fermi level falls between two band complexes and there are *precisely* enough electrons available to fill the lower set of (valence) bands and leave none in the upper set of (conduction) bands. In ionic oxides, it is common for the ions to be closed shell and the ionic solid is insulating because the individual constituents are nondegenerate and stable. For such a conventional insulator to conduct, carriers must be coerced into otherwise filled or unfilled bands of states, e.g. through doping.

A different type of oxide insulator arises when ions have partially filled shells. These transition metal compounds are known as Mott insulators and fail to conduct because (in the classical simplest picture) the energy gain from hopping between the open shell ions (roughly speaking, proportional to the bandwidth W) is outweighed by the interaction energy cost of putting an extra electron on an ion (the Coulomb repulsion U, also known as the 'Hubbard U'). In practice, there are a number of energy scales and degrees of freedom that make the behavior much more complex and interesting. For these reasons, and because they give rise to the high temperature superconductors, these Mott insulators remain, after 50 years of study, a very active field of research.

Transition metal oxides exhibit both an impressive structural variety and a rich spectrum of functionalities such as high T_c superconductivity, magnetism, ferroelectricity and colossal magnetoresistance, among many others. In a heterostructure such properties can be combined, e.g. in the search for multiferroic materials. However, perhaps a more compelling reason to study oxides is that it has become clear that novel electronic states can be realized at oxide interfaces that do not exist in the bulk phases.

Layer-by-layer growth allows synthesis of phases that are not thermodynamically stable. Recent developments of growth techniques like pulsed-laser deposition (PLD) and molecular beam epitaxy (MBE) have enabled the synthesis of oxide superlattices with atomic precision [1, 2]. These artificial 'digital' materials are currently a source of excitement both from a fundamental point of view and for future technological applications in electronics and spintronics devices because of the novel functional properties that arise. Prominent examples are the two-dimensional electron gas measured at the interface between the Mott insulator $LaTiO_3$ (LTO) and the band insulator $SrTiO_3$ (STO) [2], as well as between the two simple band insulators $LaAlO_3$ (LAO) and STO [3]. Reports of superconductivity [4] and magnetism [5] in the latter system have fueled research both on the theoretical and experimental side. Due to the emerging new functionalities and the underlying fundamental questions, *Science* magazine selected oxide interfaces as one out of ten 'runners-up' in the breakthroughs of 2007 [6]. This area of research was also featured in an editor's article in *Physics Today* [7].

Analogous to oxide surfaces [8–10] the question of polarity arises also at oxide interfaces. As we will relate in this review, symmetry breaking and charge neutrality violation at the interface play a central role in the emergence of unexpected behavior. In the perovskite structure the ionic charge is modulated along the [001] crystallographic direction, e.g. in $LaTiO_3$ positively charged $(La^{3+}O^{2-})^{+}$ layers alternate with negatively charged $(Ti^{3+}O_2^{2-})^{-}$ layers, while $SrTiO_3$ consists of formally neutral $(Sr^{2+}O^{2-})^{0}$ and $(Ti^{4+}O_2^{2-})^{0}$ layers. As shown in figure 1 a valence discontinuity arises at the (001) interface (IF) between the polar LTO and the nonpolar STO, i.e. there is $\frac{1}{2}$ electron per IF cell in excess for the formal charge states of STO to be maintained, or $\frac{1}{2}$ too little for LTO. This excess of charge corresponds to carrier densities around 3.5×10^{14}. The situation is similar in LAO/STO: at the n-type IF there is half an electron too much to keep the formal charges, while with a $SrO–AlO_2$ stacking (p-type) there is an extra $\frac{1}{2}$ hole.

During the film growth process of polar materials it is expected that the dipoles lead to a shift of the potential which increases proportional to the number of overlayers (i.e. a constant electric field) [11]. This impending 'polar catastrophe' has to be accommodated in some way. At first glance polar oxide interfaces bear similarities to polar semiconductor heterostructures. For the latter, compensation is often achieved through the so-called atomic reconstruction, where the surface/interface chemical composition is strongly altered via ordering of defects or roughening. On the other hand, at oxide interfaces an electronic reconstruction involving electron transfer into unoccupied bands can take place. Taking into account the correlated nature of the 3d electrons and the possibility of multiple valence states in transition metal ions, more complex compensation mechanisms can arise, leading to the stabilization of novel electronic phases.

Ab initio calculations play a key role in understanding the physics at oxide interfaces, but we note also that the structural complexity, the large system sizes and, last but not least, the treatment of electronic correlations pose high demands on the theoretical description. Rather than providing a full review of all theoretical work done so far, we have selected several cases that exemplify the insight that can be obtained from density functional theory (DFT) calculations, focusing on interfaces between polar and nonpolar materials. Most of the results presented here are obtained using the full-potential linearized augmented plane wave method as implemented in the WIEN2k code [13] and the generalized gradient approximation [14] to the exchange correlation potential also including correlation effects within the LDA/GGA+U method [12] (for more details the reader is referred to the original papers). Specifically, we will compare the compensation mechanisms that arise in heterostructures of the Mott insulator LTO and the band insulator STO to those comprised of the conventional ionic insulators LAO and STO. The latter is chosen both because it shows a striking variety of properties, making it by far the most studied system, and also because the remarkably intricate behavior of these rather simple materials ought to be

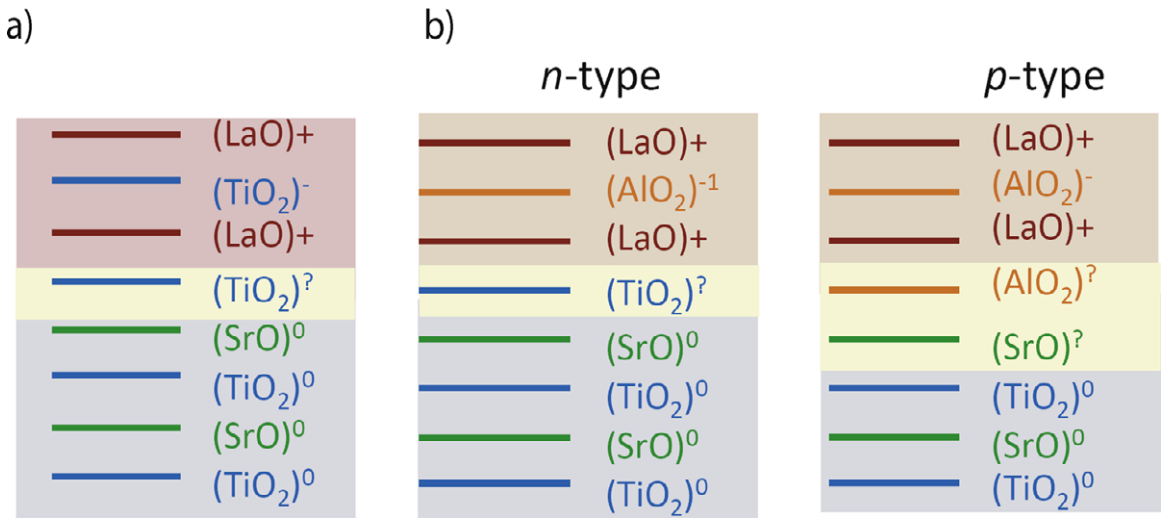

Figure 1. Schematic picture of the charge discontinuity at the (a) $LaTiO_3/SrTiO_3$ interface, as well as the (b) *n*- and *p*-type interfaces in $LaAlO_3/SrTiO_3$. Due to a mismatch of charges, the ions cannot maintain their formal valence at the interface.

understood before one deals with the additional complexity arising from the 'Mott physics' in open shell transition metal oxides. In section 2 we address the electronic properties of infinitely extended superlattices of LTO/STO and compare them to those at the isolated *n*- and *p*-type LAO/STO interfaces (sections 3.1 and 3.2, respectively). The latter are contrasted in section 3.3 with the behavior of thin LAO films on an STO(001) substrate, where we explore finite size effects and the origin of the intriguing thickness-dependent insulator-to-metal transition. In section 4 we summarize the current state of understanding of these materials and mention some future perspectives.

2. Compensation mechanisms at the $LaTiO_3/SrTiO_3$ interface

$SrTiO_3$ is a band insulator with a bandgap of 3.2 eV. Due to the well-known problem of the local density approximation (LDA) or GGA to underestimate the bandgap, the GGA bandgap separating occupied O 2p states from unoccupied Ti 3d states is 2.0 eV. In contrast, in $LaTiO_3$ the Ti 3d band is singly occupied and a strong intra-atomic Coulomb repulsion on the Ti ion leads to Mott insulating behavior. $LaTiO_3$ is one of the most studied correlated insulators. In bulk form its perovskite structure is strongly distorted, which narrows the 3d bands and thereby contributes to the Mott insulating character. The connection between the Jahn–Teller distortion and strong interaction effects in this compound is still a subject of intense research [15].

Experiments indicate that LTO grows coherently on STO. The lattice mismatch between LTO ($a = 3.97$ Å) and STO ($a = 3.905$ Å) is relatively small (2%) and produces a tetragonal distortion which breaks the t_{2g} degeneracy when LTO is incorporated into superlattices grown on STO substrates. The effect of the pseudocubic structure and the tetragonal distortion is one of the relevant issues that will be discussed in the following.

'Interdiffusion layers' of LTO/STO with sheet carrier densities in the range 10^{13}–10^{15} cm^{-2} were grown in 1996 by Yoshida and collaborators [16]. In 2002 Ohtomo *et al* [2] reported abrupt IFs involving LTO and STO demonstrating atomic control of the number of LTO layers within the STO host during the PLD process. Annular dark-field transmission electron microscopy (TEM) images indicated atomically sharp interfaces. The observed conductivity at the interface between two insulators opened up the study of polar IFs with one strongly correlated component. Electron energy loss spectra (EELS) indicated a mixed Ti^{3+}, Ti^{4+} signal close to the interface with a decay length into the STO host of the order of 1 nm, which stimulated and focused some of the early theoretical work. Subsequent studies [17–20] reported more characteristics, including nanostructures with high mobility [19] as well as samples with poor conductivity [20]. Photoemission studies of buried LTO/STO IFs found a sharp Fermi cutoff (itinerant states), becoming sharper after La $\leftrightarrow$ Sr interdiffusion due to annealing [21].

2.1. Model approaches

Before turning to the first-principles studies of this system we review briefly the results from model Hamiltonian approaches. The theoretical study of this Mott insulator–band insulator interface was initiated by Okamoto and Millis, using single-and then multiple-band Hubbard models and a statically screened Coulomb interaction ($e^2/|R - R'|$) [22]. This approach results in a complex phase diagram with ferromagnetic, antiferromagnetic and nonmagnetic solutions, as well as orbitally ordered phases in certain regimes. Employing a similar approach but an exact diagonalization for a one-dimensional chain and two-leg ladders, Kancharla and Dagotto [23] obtained that the charge disturbance extends over nine or more atomic layers away from the interface even for large interaction strength. Lee and MacDonald considered [24] again a Hubbard model with similar interactions, with new features including a Thomas–Fermi (TF) treatment of the system, and consideration of a finite system (thin film). The TF solution provided a guideline in analytic form for the minimum number of layers required to drive the electronic

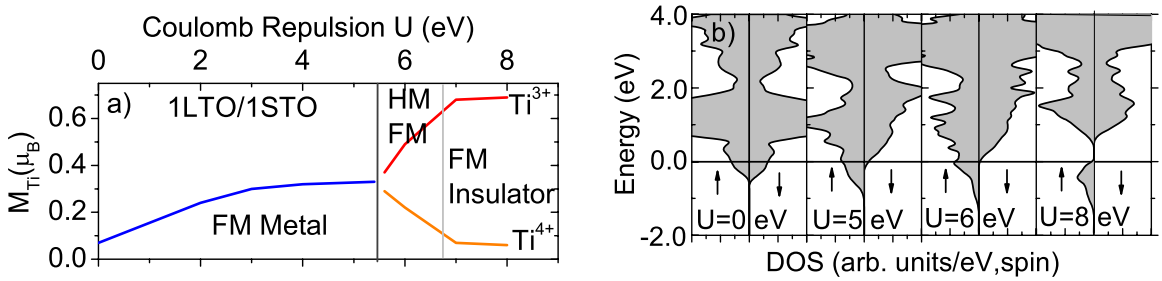

Figure 2. (a) Evolution of the magnetic moment of Ti in an LTO_1/STO_1 superlattice (SL) with a c(2 × 2) lateral periodicity as a function of the Hubbard U parameter. (b) Density of states (DOS) (arrows denote the majority and minority DOS) of the (1,1)-superlattice for different U values. A charge disproportionation occurs beyond $U \approx 5.5$ eV. HM FM denotes the region where the system shows half-metallic ferromagnetic behavior, before a Mott–Hubbard bandgap forms at around $U \approx 6.5$ eV [28].

reconstruction at the IF. More recently, Sigrist *et al* [25] have addressed similar model Hamiltonians using auxiliary boson (slave boson) mean-field theory. For (1) a correlated slab (variable interaction strength) embedded within a band insulating material ('STO') and (2) multilayers they obtained a metallic (though highly renormalized) quasiparticle behavior even in the strong interaction limit: a 2D electron gas.

2.2. DFT studies of electronic and orbital reconstruction

The odd number of electrons near the interface will give, in the local density approximation (LDA), at least one partially filled band, i.e. a metallic IF. This metallicity is likely to persist when spin polarization (LSDA) is included, though insulating solutions are, in principle, possible in LSDA. The early DFT-based studies of the LTO/STO IF adopted the LSDA (or GGA) description, necessarily obtaining metallic IFs [26, 27]. One emphasis was on the degree of confinement of the conducting layer to the IF region, which was attributed to a wedge-shaped potential due to the incorporated LaO layer [26]. Both of these studies found a decay length of roughly three unit cells: the charge is spread over several TiO_2 layers away from the interface with intermediate valent $Ti^{3+\delta}$ ions.

To model superlattices containing a Mott and a band insulator, we have adopted the LDA + U [12] (GGA + U) method as a standard approach to describe the Mott insulating nature of LTO. A variety of heterostructures were considered, where the number of LTO (n) and STO (m) layers was varied $1 \leqslant n, m \leqslant 9$. In the following we denote these superlattices by LTO_n/STO_m. To describe the antiferromagnetic (AFM) G type coupling of LTO (rocksalt arrangement of the Ti spins), but most importantly, to allow more complex electronic reconstructions and magnetic order, the lateral cell was enlarged to c(2 × 2) or p(2 × 2).

The initial question that arises is the appropriate value of the on-site repulsion parameter (Hubbard) U to choose. Calculations for an undistorted LTO crystal in a tetragonal set-up (to model the magnetic coupling) show that a value of $U = 8$ eV and intra-atomic Hund's $J = 1$ eV are needed to obtain an AFM-G type insulator. This value is somewhat higher than the one generally used for titanates with a distorted perovskite structure [31].

For an LTO_1/STO_1 superlattice (which, in fact, corresponds to one type of double perovskite compound), we have

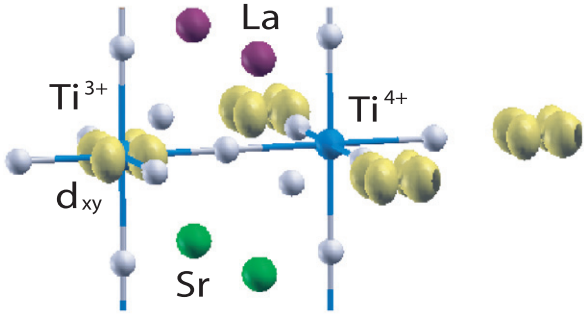

Figure 3. Spatial distribution of the electron density integrated between −2 eV and E_F showing the charge and orbitally ordered state at the LTO/STO interface. For $U = 8$ eV Ti^{3+} and Ti^{4+} order in a checkerboard arrangement with an occupied d_{xy} orbital at the Ti^{3+} sites and no charge at the Ti^{4+} sites.

investigated how the value of U influences the behavior of the Ti ion. As shown in figure 2 for $U = 0$ a small moment of ≈0.07 μ_B arises on the Ti ions. With increasing U up to 5 eV the magnetic moments of the two equivalent Ti ions at the interface increase and saturate at 0.33 μ_B. In this region the system is a ferromagnetic (FM) metal. However, beyond this value charge disproportionation emerges, making the system a ferromagnetic half-metal for 5 eV $< U <$ 7 eV, before a bandgap opens up for $U >$ 7 eV separating the lower Hubbard band from the unoccupied 3d states. In the strong interaction regime a layer of Ti^{3+} and Ti^{4+} ions ordered in a checkerboard arrangement emerges at the interface. As shown in figure 3 the extra electron at the Ti^{3+} sites occupies the d_{xy} orbital. This is not true orbital ordering because the Ti ion lies at the IF and the lowered symmetry breaks the degeneracy of the t_{2g} orbitals, with d_{xy} lying lowest. The local Ti^{3+} moment, reduced by mixing with oxygen as is common in oxides, is 0.72 μ_B; the total moment per IF cell including the induced moment on the O ion is enforced by the FM insulating state to be 1 μ_B. Finally, an antiferromagnetic coupling between Ti^{3+} within the interface layer becomes energetically favored [28].

This LTO_1/STO_1 heterostructure is, however, more a synthetic compound than a periodic array of interfaces. To determine the compensation mechanism and relaxation length towards bulk behavior at an isolated interface, we have studied more extended superlattices. The change in the electronic structure across an LTO_1/STO_5 multilayer with *ideal positions*

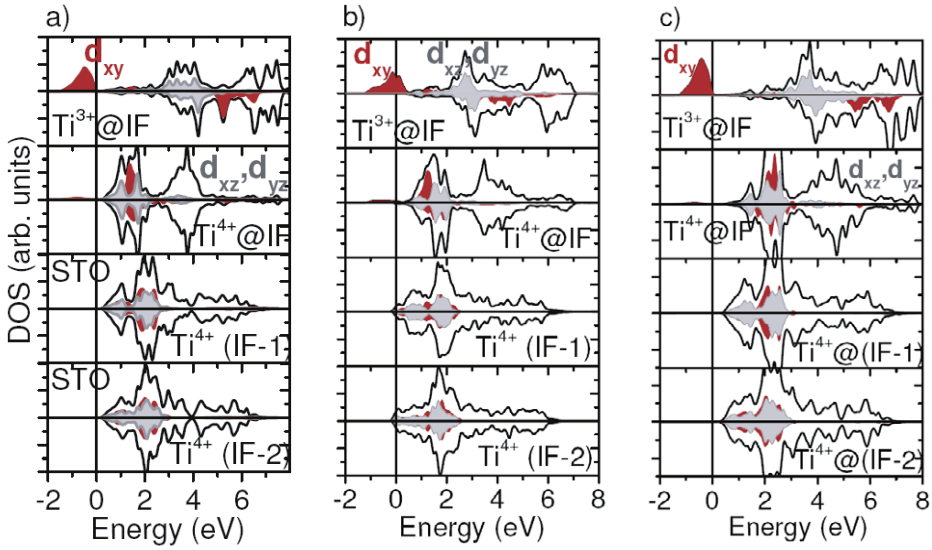

Figure 4. Layer-resolved projected DOS of the Ti 3d states in the LTO_1/STO_5 heterostructure with ideal (a) and relaxed positions of the ions (b) within GGA and (c) within GGA + U. For the structure relaxed within GGA the excess charge leaks into the STO host [28], while relaxation within GGA + U stabilizes further the charge and orbitally ordered state at the interface.

of the atoms is displayed in figure 4(a). Within GGA + U, the charge mismatch is accommodated essentially entirely in the IF layer which contains charge ordered Ti^{4+} and Ti^{3+}. The Ti^{4+} ion in the next layer on the STO side has a projected density of states that is nearly identical to that of bulk STO. Analogously, Ti^{3+} ions one cell away from the IF in a superlattice with a thicker LTO part (LTO_5/STO_5—not shown here) is similar to that of bulk LTO. Small differences between Ti^{4+} and Ti^{3+} ions in the IF layer and their counterparts in the bulk can be attributed to the different environments.

Hamann *et al* [27] and Okamoto *et al* [29] pointed out the importance of the structural relaxations on the electronic properties. This strong electron–lattice coupling has become essential to understand the behavior near IFs involving polar discontinuities. GGA [27] and LDA + U [29] calculations within a p(1 × 1) unit cell predict a strong ferroelectric distortion of 0.15 Å in the interface TiO_2 layer, leaving the Ti–Ti distance across the LaO layer larger than the Ti–Ti distances within the STO slab. The lattice distortion quickly decays away from the IF into the STO host. As shown in figure 4(b) these lattice relaxations invoke small but nonetheless important band shifts compared to the ideal structure: the occupied Ti d_{xy} state (the lower Hubbard band) rises by 0.3–0.4 eV, closing the very small gap and leading to partially filled bands and conducting behavior. A small concentration of holes are introduced into the d_{xy} band, with the compensating electrons going into deeper layers in the STO slab in Ti orbitals of d_{xz}, d_{yz} character. This orbital occupation is sustained even at the GGA level [30]. Within GGA + U the IF layer of Ti ions remains charge ordered and magnetically ordered, in spite of the ∼30% occupation of holes in the band and a reduction of the magnetic moment at Ti^{3+} to 0.49 μ_B. Overall, the lattice polarization obtained within GGA redistributes and smooths the charge profile, resulting in a larger relaxation length towards bulk behavior in the STO host [27, 29].

On the other hand, a structural relaxation within GGA + U taking into account a larger c(2 × 2) lateral periodicity results in quite a different electronic behavior. While the vertical relaxations are slightly weaker than within GGA, a lateral relaxation of the oxygen ions away from the Ti^{3+} sites (breathing mode) leads to a further stabilization of the charge and orbitally ordered state. Moreover, the splitting between the occupied Ti d_{xy} orbital and the rest of the t_{2g} states is enhanced, leading to a larger bandgap as displayed in figure 4(c).

This charge and orbitally ordered phase at the LTO/STO interface results from the interplay of electronic correlations and additional degrees of freedom and is an example how these can lead to unexpected compensation mechanisms of the interface polarity involving novel electronic states.

Since x-ray diffraction experiments [18] indicate only a tetragonal (and not orthorhombic) distortion for the epitaxial LTO layers in these heterostructures, an important issue is whether LTO can preserve its insulating character without the $GdFeO_3$-type distortion of the bulk compound. The question of the (non)conducting character of pseudocubic LTO has been addressed by Ishida and Liebsch [32] using a LDA + DMFT (dynamical mean-field theory) method including the Ti 3d states and treating the on-site interaction with exact diagonalization techniques. For tetragonal LTO appropriate to model the growth on STO, they obtained a metal–insulator transition in LTO at $U = 6$ eV ($J = 0.65$ eV). This critical value of U is not much different than what we obtained from GGA + U. However, assuming that $U = 5$ eV is more appropriate for Ti, the authors conclude that tetragonal LTO itself is metallic, and that this accounts for the conducting LTO/STO multilayers that are observed experimentally. Using this value of U and treating $(LTO)_3/(STO)_4$ multilayers, they find that some of the Ti charge in LTO is transferred into the STO layers. Since the Fermi level of LTO must lie within the STO gap, this leaking of charge into STO would be like the

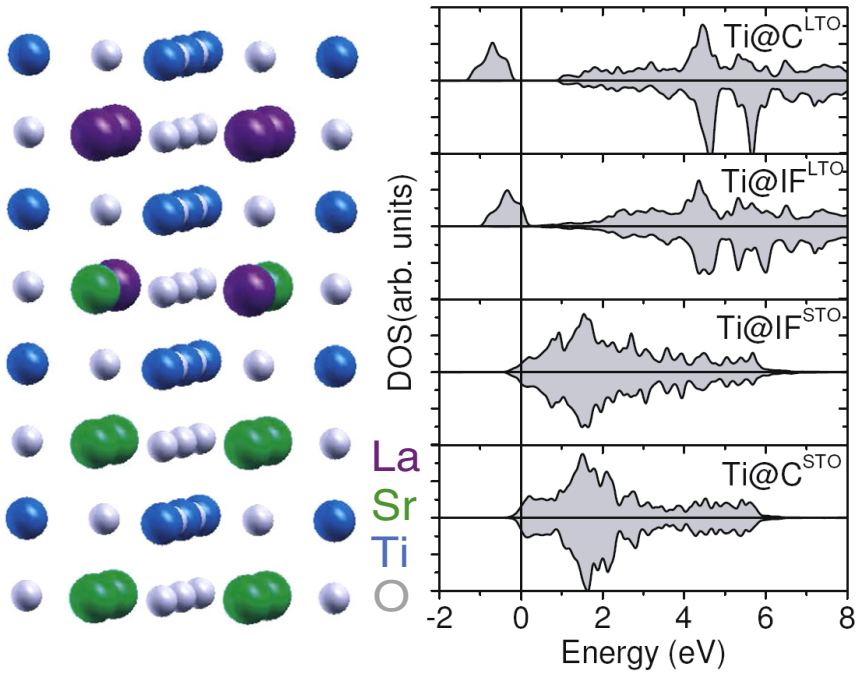

Figure 5. Layer-resolved projected DOS of the Ti 3d states in the LTO_2/STO_2 heterostructure with an intermixed La, Sr layer, pictured at the left. In the central Ti layer of the LTO slab, Mott insulating behavior is retained. The LTO side of the interface can be considered as a slightly (hole-) doped Mott insulator, and compensating electrons must lie in the conduction bands on the STO side of the interface.

'metal-induced gap states' that are well studied in conventional metal–semiconductor IFs.

2.3. Compensation through La and Sr intermixing

Besides the possibility of an electronic reconstruction, we have also considered an atomic reconstruction through an intermixed (La, Sr) layer. The projected DOS of a superlattice containing two unit cells of LTO and STO with one mixed La, Sr layer at the interface is shown in figure 5. While Ti ions on the LTO side of the interface behave nearly as in the Mott insulating bulk material, the Fermi level crosses the d_{xy} band of Ti^{3+} next to the interface. The t_{2g} bands of Ti^{4+} on the STO side have also a small occupation, leaving the system conducting. This is possibly related to the fact that solid solutions of LTO and STO (LSTO) are conducting even for small doping concentrations of Sr [33, 34] in LTO, or La in STO.

The implications of strong electronic correlations at the LTO/STO IF have certainly not been completely resolved. It is also important that more widely spaced IFs be studied to corroborate the results on the isolated IF. In the meantime, however, the limelight and the effort have both been concentrated on the LAO/STO system, which we will discuss in section 3.

3. Compensation mechanisms in the $LaAlO_3/SrTiO_3$ system

At an LAO/STO interface both the A and the B cations change across the interface, leading to two distinct types of interfaces: the electron-doped *n*-type interface with an LaO layer next to a TiO_2 layer and the hole-doped *p*-type interface where an SrO layer lies next to an AlO_2 layer (see figure 1). The interest in this system was triggered by experimental findings that the *n*-type interface between these two band insulators is conducting, while the *p*-type interface was reported to be insulating [3]. The high electron mobility (10^5 cm^2 V^{-1} s^{-1}) and carrier density[3] ($\sim 10^{17}$ cm^{-2}) initially reported for the *n*-type interface suggested possible applications in oxide-based electronic devices and invoked a surge in both theoretical and experimental studies. In later studies, however, it became clear that growth conditions during the PLD process play a decisive role and that the unusually high carrier density is rather related to the formation of oxygen vacancies during the deposition process [11, 35–38]. This *extrinsic* conductivity has a predominantly 3D character [39]. Increasing the oxygen partial pressure during growth or subsequent annealing in an oxygen atmosphere leads to an increase in sheet resistance by several orders of magnitude. In fact, the three functional properties observed so far can be related to three different regions of oxygen pressure [40]: (3D) conductivity at $p_{O_2} \sim 10^{-6}$ mbar and superconductivity at $p_{O_2} \sim 10^{-4}$ mbar [4], while magnetic effects [5] are observed at $p_{O_2} \sim 10^{-3}$ mbar.

Many of the theoretical studies so far have focused on the origin and type of carriers at the interface leading to conductivity. The formal charge mismatch at the polar interface means that there will be too many (*n*-type interface) or too few (*p*-type interface) electrons to satisfy the formal charges, so there must be potential carriers in the interface regions. As just discussed, the initially measured conductivity is extrinsic in nature. Films grown at 'high' oxygen pressures, where the effect of oxygen defects is minimized, are (nearly)

[3] Note that the intrinsic carrier density scale of one-half carrier per interface cell is equal to 3×10^{14} cm^{-2}.

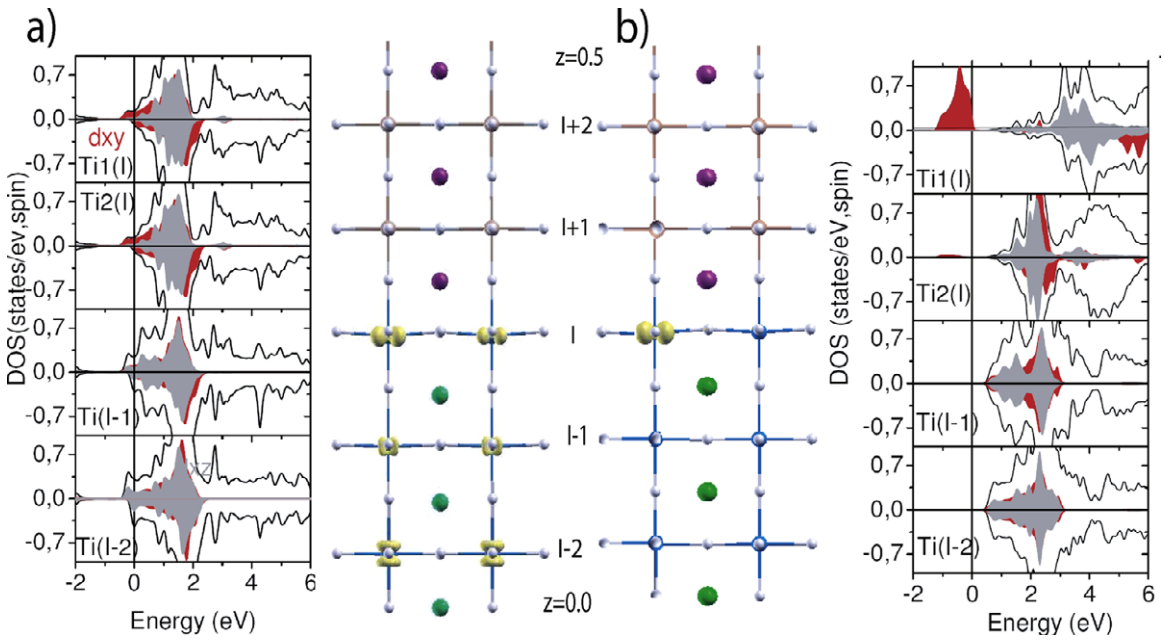

Figure 6. Layer-resolved DOS obtained within GGA + U showing the Ti 3d bands and side views of the $LAO_{4.5}/STO_{5.5}$ superlattice, relaxed within (a) GGA and (b) GGA + U. The side views also display the spatial distribution of the occupied 3d orbital at the Ti sites. Structural relaxation within GGA + U leads to two distinct Ti sites at the interface: Ti^{3+} and Ti^{4+}, while the GGA geometry results in two identical Ti ions in the IF layer and finite occupation of Ti 3d states in deeper layers [45].

insulating at low temperature. The fact that carriers seem to become localized at low temperature is a more challenging result to explain than if they were simply free and conducting. We restrict our discussion to this regime of defect-free heterostructures where the influence of oxygen vacancies can be neglected.

3.1. The n-type $LaAlO_3/SrTiO_3$ *interface*

In order to model the *n*-type interface most studies have adopted multilayers containing two inversion symmetric *n*-type interfaces to avoid the formation of a net dipole in the slab with its resulting spurious electric field. From electron counting one expects that the odd number of electrons per interface cell must give a metallic result within LDA. This was confirmed for both *n*-type and *p*-type IFs [41–43]. Gemming and Seifert [41] found the 'excess' charge for either *n*- or *p*-type interfaces to be rather strongly localized to within a couple of layers of the interface and that the metallic state can be canceled by adding a background charge. The dielectric properties determined from linear response theory show a strong dependence not only on strain but also on the local interface chemistry. Popovic *et al* [44] investigated more extended superlattices with the *n*-type interface and, also after relaxation, concluded that the interfacial charge extended several layers away from the interface layer. This study noted multi-subband occupation, with some electrons remaining localized at the interface while other bands contained more delocalized electrons. This aspect will be discussed in more detail below.

Because the LaO–TiO_2 layers at the *n*-type interface constitute the building block of the Mott insulator LTO, we have considered the role of correlation effects also in this case. Indeed, the resulting compensation mechanism is very similar to the one in LTO/STO superlattices with a charge disproportionation into a charge (CO) and an orbitally ordered (OO) state with Ti^{3+} and Ti^{4+} ordered in a checkerboard arrangement [42].

The role of lattice relaxations has been investigated considering more isolated interfaces in an $LAO_{4.5}/STO_{5.5}$ superlattice (with $a_{\parallel} = a_{STO} = 3.91$ Å) shown in figure 6 [45]. The lattice relaxation was performed separately within GGA and GGA + U. The main characteristic, common to both, is a strong polarization in the layers close to the interface, predominantly in the STO part of the heterostructure, whereas in the LAO layer next to the IF both cations and anions shift by similar amounts. Analogous to the LTO/STO interface (see section 2) a strong buckling in the interface TiO_2 layer by 0.17 Å (GGA) and 0.12 Å (GGA + U) is found. The precise value of lattice polarization at the interface varies slightly with the separation between the interfaces and the lateral lattice parameter [41, 43, 47].

While the atomic displacements within both approaches show similar trends, they have somewhat higher absolute values within GGA. Still, subtle differences (e.g. a small lateral shift of the oxygens away from the Ti^{3+} ions within GGA + U) result in a completely different electronic behavior for the GGA + U and the GGA geometries. For the former the charge and orbitally ordered state is further stabilized and the charge is strongly confined to the interface layer (see figure 6(b)) [45]. Zhong and Kelly [48] have addressed further symmetry lowering due to rotations/tilting of the octahedra that narrow the Ti 3d band and found that these are energetically favorable even within LDA. Including correlation effects with the LDA + U method, they obtain a similar charge disproportionation, orbital reconstruction and AFM coupling of the spins in the strong interaction limit.

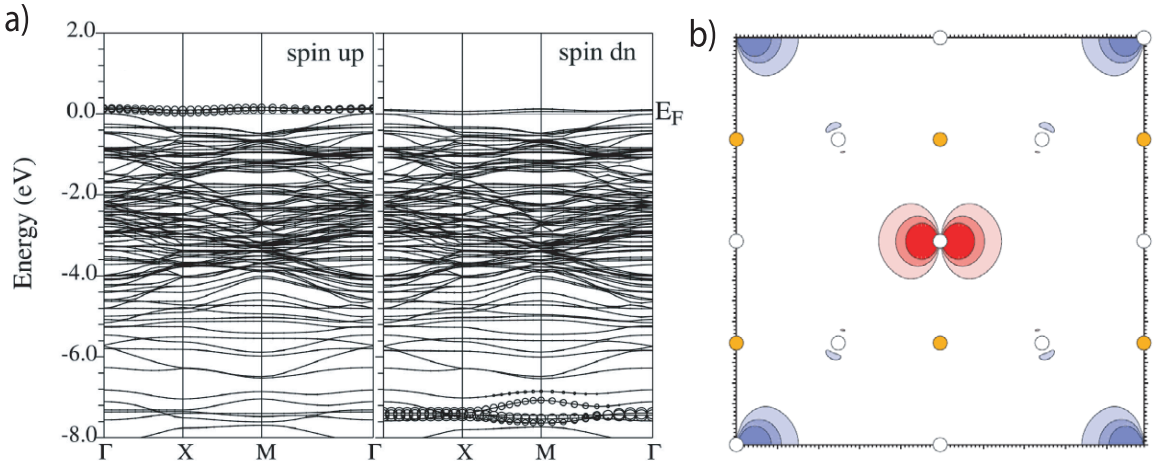

Figure 7. O π-holes at the p-type LAO/STO interface in a p(2 × 2) cell within GGA + U: (a) band structure, showing the strongly localized upper Hubbard band at the Fermi level, and (b) spatial distribution of the antiferromagnetically coupled holes in the AlO_2 IF [42].

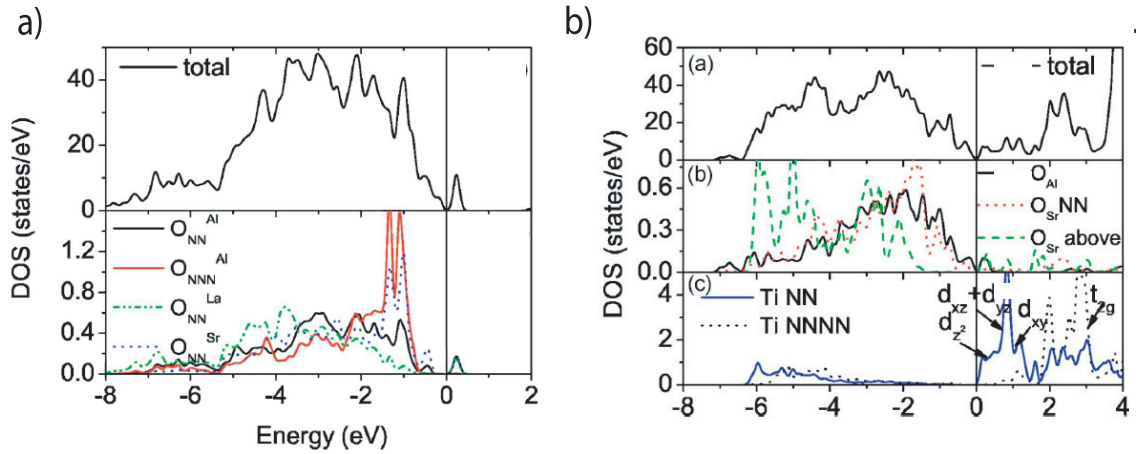

Figure 8. DOS of the p-type LAO/STO IF with an oxygen vacancy in the (a) AlO_2 layer and (b) SrO layer; in (a) the unoccupied states above the Fermi level have O 2p character and are localized at the neighboring oxygen ions around the vacancy, while in (b) they are mainly due to Ti 3d bands of the underlying TiO_2 layer [42].

In contrast, for the GGA geometry the excess charge is redistributed over the STO part of the $LAO_{4.5}/STO_{5.5}$ heterostructure (see figure 6(a)). While CO is nearly suppressed, there is a residual orbital ordering with an occupation of the d_{xy} orbital of Ti in the interface layer, while in more distant layers the d_{xz} and d_{yz} orbitals are occupied. Analyzing the band structure, Popovic *et al* found [44] that the latter bands have a very small dispersion and lie a bit higher than the bottom of the dispersive d_{xy} band (at $\vec{k} = 0$). The authors proposed that only the latter contributes to the transport properties of the system. This gives a possible explanation that the measured carrier densities are one order of magnitude lower than the expected 3.5×10^{14} cm^{-2}.

Still the CO/OO solution corresponds to the ground state (favored by 0.45 eV). For the samples grown at high pressures the sheet resistance is seven orders of magnitude higher and shows an upturn at low temperatures which is consistent with CO or polaronic behavior. Electron delocalization at higher temperatures may lead to the behavior described in figure 6(a).

Several studies have addressed the band offsets at the n-type LAO/STO interface. Depending on the applied method—the reference potential method [62], the O 1s core levels [45, 44], the local density of states or the macroscopic averaging technique [46]—there are notable differences (e.g. the calculated valence band offset varies between 0.1 and 0.9 eV). In general, the STO bandgap lies completely within the LAO gap, implying that charge carriers of either sign (electrons or holes) will go into the STO side of the interface.

To determine the confinement of the electron gas at the interface, Janicka *et al* [49] have considered superlattices containing 23 MLs of STO and 1–5 layers of LAO. These GGA calculations determine a relaxation length of ∼1 nm. Using the O 2s states to probe the band bending and the calculated bandgap of bulk STO, these authors conclude that electrons 5 ML away from the interface occupy a classically forbidden region, forming so-called metal-induced gap states.

3.2. *The p-type* $LaAlO_3/SrTiO_3$ *interface*

The p-type LAO/STO interface which was found to be insulating despite the charge mismatch has been less studied. The initial reports of Ohtomo and Hwang [3] suggested that

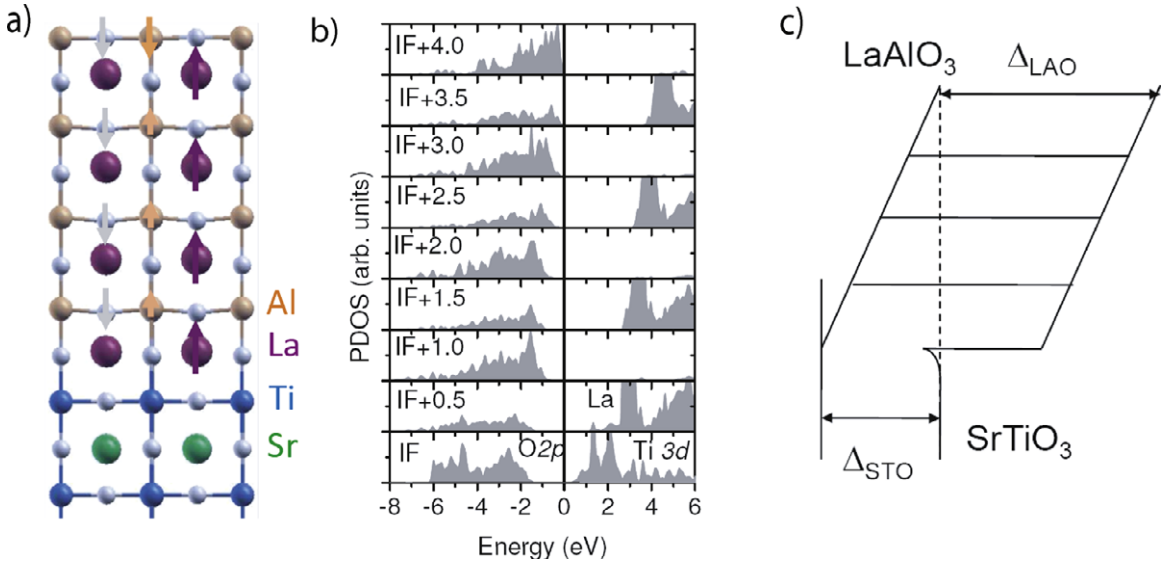

Figure 9. (a) Side view of the relaxed structure of 4 MLs LAO/STO(001) showing a strong polar distortion of the LAO film dominated by a 0.2–0.3 Å outward relaxation of La^{3+} (purple atoms) and additional buckling in the subsurface AlO_2 layers; (b) layer-resolved density of states of 4 ML LAO/STO(001) with relaxed positions of the cations. The strong lattice polarization allows the system to remain insulating (here $E_g = 0.4$ eV) until a crossover to an electronic reconstruction takes place at around 5 MLs of LAO/STO(001) [52]. (c) Schematic figure of the electric field induced linear shift in band edges in LAO/STO(001).

the interface is structurally perfect, i.e. without appreciable defects. For such an interface LDA/GGA gives a metallic solution with the Fermi level crossing the O 2p band [42, 43]. Since the occupied Sr and Al states lie well below the Fermi level, the only possibility to obtain insulating behavior (assuming a defect-free heterostructure) is to consider correlation effects at the O 2p orbitals. Applying a Hubbard repulsion U on the O 2p states with a single hole present amounts to a lifting of the orbital degeneracy of the O 2p band. Considering the charges and geometry of Al and O in the AlO_2 layers, it is likely that the holes will go into π-bonds. Indeed the GGA + U treatment results in a localization of a significant part of the hole on a central oxygen with some contribution of the nearest neighbors, while the next-nearest neighbors are not affected (see figure 7(b)) and have a fully occupied O 2p band. The holes are spin-polarized and the degree of localization of charge is enhanced for antiferromagnetic coupling. However, as shown in figure 7(a), the upper Hubbard band is pinned at the Fermi level with some admixing of O in the next SrO layer. These calculations [42] were performed for superlattices with ideal positions of the atoms where the two inversion symmetric interfaces are rather close. Including lattice relaxations and a better separation between the interfaces is likely to lead to an insulating polaronic solution.

In later experiments [11] it became clear that oxygen vacancies play a significant role at the p-type interface. We have considered also this more obvious possibility and find that indeed the Fermi level lies in a dip of the DOS both for a vacancy in the AlO_2 and the SrO layer [42]. However, states are observed immediately above the Fermi level and these have different character for both cases. In the former (figure 8(a)) they result from the neighboring oxygens around the vacancy, while in the latter (figure 8(b)) they are 3d states of the Ti ion whose apex oxygen is missing. In both cases the vacancies are likely to lead to F centers.

Park *et al* [43] have also addressed the electronic behavior at the p-type as a function of the oxygen vacancy concentration, finding that a system with 25% vacancies in the SrO layer is metallic, while 50% results in a small bandgap. We note that the concentration of oxygen vacancies is rather high, but consistent with the 32% estimated from experiment [11].

3.3. Thin $LaAlO_3$ *films on an* $SrTiO_3$*(001) substrate*

Recent experiments on thin LAO films deposited on an STO(001) substrate revealed a significant thickness dependence of the transport properties [50]: the system switches from insulating to conducting behavior between 3 and 4 monolayers (MLs). Moreover it was shown that metallic behavior can be induced by an external bias even below the critical thickness of 4 MLs and that conducting and insulating regions can be 'written' by an atomic force microscope tip [51]. At first glance these results do not fit in the picture obtained from the DFT calculations for extended LAO/STO superlattices discussed in section 3.1. In the latter case the compensation mechanism at the n-type interface is rather local, involving partial occupation of the Ti 3d band, independent of the thickness of the LAO or STO layer.

In order to explore the effect of the surface on the interfacial properties we have performed DFT calculations within GGA for 1–5 MLs of LAO on an STO(001) substrate. These are modeled in the supercell geometry with two inversion symmetric surfaces on both sides of the slab to avoid spurious electric fields. The surfaces are separated from their periodic images by a vacuum region of ∼10 Å. In the following we will discuss the role of the lattice relaxations and their implications for the electronic properties.

3.3.1. Ionic screening of the electric field. As discussed in the previous sections, in the LTO/STO and LAO/STO superlattices the ferroelectric distortion is most pronounced in the $SrTiO_3$

part of the system with a significant buckling of the interface TiO_2 layer. In contrast, for the thin films the strongest ionic displacements are observed in the $LaAlO_3$ film. In all cases the surface AlO_2 layer relaxes inward with similar values for oxygen and Al, while the subsurface layers show a strong and uniform lattice polarization, dominated by an outward relaxation of La of 0.2–0.3 Å and buckling in the AlO_2 layers. The relaxation pattern for a 4 ML film is shown in figure 9(a). Using the formal ionic charges we can make a rough estimate of the dipole shift resulting from the polar distortion. We note that these dipole moments include only the ionic part and no contributions due to electron cloud polarization. Indeed, the obtained trend is surprisingly uniform with a layer-resolved dipole moment of ∼0.55 and ∼0.75 eÅ in the AlO_2 and LaO layers, respectively, and a vanishing dipole moment in the surface AlO_2 and interface TiO_2 layers. Adding these contributions for a 4 ML LAO film on STO(001) results in a total ionic dipole of 4.8 eÅ, which is 60% and of opposite sign to the bare dipole of the polar LAO film. Thus, the lattice relaxation plays an important role in reducing the electric field generated by the polar LAO film.

3.3.2. Finite size effects: thickness-dependent insulator-to-metal transition. The lattice polarization in the LAO film also has a significant impact on the electronic properties: while all systems with bulk positions of the ions show metallic behavior, below the critical thickness the strong lattice polarization allows the system to remain insulating, preserving the bulk charge states of the ions. The bandgap that opens up upon relaxation of the structure amounts to 1.7 eV for 1 ML LAO/STO(001) but decreases steadily (by ∼0.4 eV/ML with each added layer). Finally, at an LAO film thickness of around 5 ML the bandgap collapses and a crossover to an electronic reconstruction takes place. In order to gain insight in the underlying mechanisms we have plotted in figure 9(b) the layer-resolved density of states for 4 ML LAO/STO(001). The rigid upward shift of the O 2p bands as they approach the surface reflects the strong electric field of the LAO film. In this system, which still has a bandgap of 0.4 eV, the valence band maximum is determined by the top of the O 2p band in the surface layer, while the conduction band minimum is at the bottom of the Ti 3d states. The electronic reconstruction that emerges beyond 5 MLs of LAO is due to the overlap of these two bands, resulting in a finite occupation of the Ti 3d band and some holes in the surface O 2p band. As shown in the schematic picture (figure 9(c)) the potential build-up due to the polar LAO layer causes charge transfer into the narrow bandgap STO. This mechanism is intriguing, because it suggests two types of carriers that are spatially separated—holes localized in the surface layer and electrons in the interface layer. Further analysis of the band structure reveals that the band overlap is also indirect in reciprocal space with the bottom of the Ti d_{xy} band at the Γ-point and the top of the valence O 2p band being at the M-point. Recent x-ray adsorption spectroscopy measurements have confirmed that the d_{xy} orbital is the lowest available state for conduction electrons [53]. We note, however, that the total carrier density just beyond the critical thickness is an order of magnitude lower than the expected 3.5×10^{14} cm^{-2}, as also found from hard x-ray angle-resolved photoelectron spectroscopy [54], but increases continuously with each added layer [55, 56].

The thickness-dependent insulator-to-metal transition was also addressed by Ishibashi and Terakura [57] exploiting the recently proposed Coulomb cutoff technique [58] for eliminating any direct Coulomb-interaction-based coupling between supercells and their periodic images. In their calculations the transition to metallic behavior was obtained already at four overlayers of LAO instead of five as in our calculations; this may reflect a ∼0.2 eV difference in potential rise across the LAO slab, part of which may easily be due to small differences in the atomic relaxations. It is worth mentioning that, depending on set-up (see discussion in section 3.4), the choice of exchange correlation potential (LDA versus GGA), differences in the lateral lattice constant and the resulting atomic relaxations, the calculated critical thickness for the insulator-to-metal transition varies from 3 to 6 MLs [52, 57, 51, 59–61]. The predicted critical thickness is likely to be affected also by the bandgap underestimation typical for LDA/GGA.

Due to the small occupation of the Ti 3d band after electronic reconstruction sets in, the properties are less influenced by correlation effects compared to the isolated interface. Lee and Demkov [62] have studied 3 and 5 ML LAO on STO(001) using LDA + U with $U_{\text{eff}} = 8.5$ eV. They find in the latter case a charge transfer exclusively in a split-off Ti state of d_{xy} character in the interface layer. The pseudo-Jahn–Teller effect is discussed as indication of a strong electron–phonon coupling and a possible origin of superconductivity. Breitschaft *et al* [63] argue that the shape of scanning tunneling spectroscopy curves is better described using $U = 2$ eV and that the system shows a two-dimensional electron liquid behavior.

An interesting question is whether holes contribute to the conductivity and whether they can survive in the surface layer or whether other mechanisms—e.g. oxygen vacancy formation—can eliminate them. Cen *et al* [51] have addressed surface vacancies in a 3 ML LAO/STO(001) film, showing that when the surface AlO_2 layer is compensated by vacancies, the interface layer becomes metallic with a finite occupation of the Ti 3d band. Moreover, the compensation of the surface layer through oxygen vacancies also removes the upward shifts of the oxygen 2p bands. Willmott *et al* addressed the possibility of interdiffusion at the interface by including an LTO layer at the *n*-type interface [64]. This leads also to a metallic state with an enhanced occupation of the Ti 3d band at the interface. These results show that the properties at the interface can be affected in important ways by the precise termination, stoichiometry and chemical composition of the surface and interface, thus opening paths to manipulate the electronic behavior of the system.

Thin LAO films with a p-type interface: Ishibashi and Terakura [57] found that five layers of LAO over a *p*-type IF remain insulating (recall that five layers over the *n*-type IF is metallic due to band overlap). Thus there is definitely asymmetry for the two types of IFs in this system. They also found that, if no atomic relaxation was done (ideal geometries

were used), then *every case* was metallic; the electronic system and its screening alone cannot sustain the formal ionic charges in such heterostructures. The analysis of electronic screening in this system reveals a local response that is virtually impossible to obtain by experiment. This initiates an important area of study that needs to be continued and extended to gain a fundamental understanding of these heterostructures.

3.4. Superlattices with coupled interfaces

As we have seen in section 3.3, deposition of polar LAO films on nonpolar STO(001) results at some point—around four layers in the LAO/STO system—in an electronic reconstruction, which from theoretical studies so far involves a simultaneous electronic reconstruction at the interface and the surface. Experimental probes have not yet established this scenario with certainty.

There is a (somewhat) larger scale version of this issue that merits attention: one can consider the repeated growth of alternating *n*- and *p*-type interfaces [35]. The corresponding supercell has no inversion or mirror symmetry; it is polar and has a dipole. In such a case the polarization catastrophe is again an issue, but with an increased distance scale: the repeat distance is the supercell dimension rather than the unit cell dimension. Calculations of such LAO/STO superlattices containing alternating p and n interfaces have been reported, and they also show thickness-dependent phenomena: while LAO_4/STO_4 superlattices were insulating after structural relaxation [43, 41], LAO_n/STO_n beyond $n = 8$ were conducting [65]. Analogous to the thin films, the reconstruction involves electron carriers at the *n*-type interface and hole carriers at the *p*-type interface and transfer between them. These calculations on asymmetric systems/cells raise some conceptual questions about the physical behavior, and also the simulation.

The polar nature of oxides (LAO and LTO in the cases discussed here) led early on to questions about how the experimental heterostructures should be simulated in calculations. To model *isolated* IFs it has been the practice to use (as mentioned above) symmetric supercells, i.e. two opposing *n*-type IFs in the supercell. Then there is, by symmetry, no dipole in the cell and a periodic supercell treatment is appropriate. In the study of finite overlayers computational practices have varied. Again, the use of symmetric supercells is straightforward; each half of the cell may have a dipole as determined by the geometry and the (self-consistent) response to electric fields while the opposing dipoles leave a slab that can be treated in a periodic supercell.

This approach makes the cells twice as large and enhances significantly ($\sim 2^3 = 8$) the computational cost, which is an important practical issue. Finite slabs [59] or repeated opposing *n*- and *p*-type IFs without inversion symmetry [65] have also been used to model such situations. In such cases the imposition of periodicity on the potential results in an internal electric field in the STO side of the slab that is comparable in magnitude to that in LAO and opposite in sign [65]. Son *et al* have also modeled asymmetric slabs [55], employing a 'dipole correction' that has been devised [66, 67] for finite slabs to correct for the imposed periodicity. The superlattices containing exclusively *n*-type interfaces and those with alternating *n*- and *p*-interfaces correspond to two distinct physical situations. Still, the question remains as to what extent these can be realized experimentally taking into account possible asymmetry due to roughness and/or defects. The comparison of various methods and comparison with experiment needs further consideration to obtain a reliable physical picture.

4. Modeling oxide interfaces: summary and perspectives for the future

In summary, first-principles calculations suggest that at an interface between a polar and a nonpolar material different compensation mechanisms may be at work, depending on some rather detailed features. For infinitely extended superlattices of the Mott insulator LTO and the band insulator STO and in superlattices containing *n*-type LAO/STO interfaces, the ground state is a charge and orbitally ordered Ti^{3+}, Ti^{4+} layer with an occupied d_{xy} orbital at the Ti^{3+} sites. Structural relaxation within GGA + *U* including a larger lateral periodicity leads to a further confinement of the excess electron at the interface. On the other hand, relaxation within GGA within a p(1×1) lateral unit cell leads to a delocalization and redistribution of the charge throughout the STO part of the superlattice (overscreening), significantly increasing the confinement length of the electron gas. This scenario is likely to happen at higher temperatures when electron hopping is possible.

In contrast, a completely different situation arises in thin LAO films on an STO(001) substrate. Here a strong and uniform lattice polarization leads to an insulating behavior for a few LAO layers. However, the potential build-up with each added LAO layer invokes a reduction of the bandgap and finally an insulator-to-metal transition and an electronic reconstruction but with a much lower carrier density than expected from formal electron counting. We note that the finite size effects are not restricted to LAO films on STO but has also been reported experimentally, for example, for LVO/STO(001) [69, 70].

Recent measurements of Hwang *et al* [68] show that thin LAO films (5–10 MLs) exhibit metallic temperature dependence, while thicker films (up to 25 MLs) show an upturn of the sheet resistance at low temperatures. These findings seem to support the DFT results, suggesting a coupling of surface and interface in the thinner films and an interface-confined compensation mechanism at more isolated interfaces possibly connected with localization and charge ordering.

The electronic behavior in thin LAO is likely to be very sensitive to defects and adsorbates. DFT calculations [51] give indications that oxygen vacancies can cancel the potential build-up observed in shifts of the O 2p bands in the non-defective films. Moreover, adsorbates or a nonpolar oxide layer [71] can modify significantly the properties of the system. Thus, finite size effects (film thickness) together with a number of further parameters (e.g. defects, adsorbates, an oxide overlayer or an external bias) can be used to tailor the interfacial properties and need further attention in future.

In this review we have concentrated on systems where the charge mismatch is due to a d^1–d^0 occupation across the interface, and we have seen that electronic correlations can lead to novel compensation mechanisms unanticipated from semiconductor heterostructures. These processes open the possibility of realizing novel charge, orbital and magnetically ordered states. A further degree of complexity arises when both transition metal ions across the interface contain d electrons and, for example, the valence mismatch across the interface is enhanced. The competition between these ions to compensate the charge mismatch at the interface may result in complex orbital physics and promises to lead to a plethora of new electronic phases. Obtaining a fundamental understanding of the phenomena that arise at polar transition metal oxide interfaces could lead to novel concepts for oxide-based electronics devices.

While we have considered here oxide heterostructures with perovskite structure, analogous effects can also arise in other systems. An example for a polar interface where the constituents have a corundum-derived structure is the hematite–ilmenite system. A stacking of $2Fe^{3+}/3O^{2-}$ layers in hematite and $2Fe^{2+}/3O^{2-}/Ti^{4+}$ in ilmenite results in a polar discontinuity across the Fe_2O_3–$FeTiO_3$ interface. DFT calculations including an on-site Coulomb correction [72, 73] give theoretical evidence for the lamellar magnetism hypothesis [74]: a mixed Fe^{2+}, Fe^{3+} contact layer is formed to accommodate the charge mismatch. The uncompensated moments in the interface layer give rise to ferrimagnetism at the interface between the canted antiferromagnet Fe_2O_3 and the room temperature paramagnet $FeTiO_3$. This interface-induced magnetism makes this system interesting, e.g. for spintronics applications.

Unanticipated phenomena can arise also in heterostructures without a polar discontinuity. For example the confinement of the electrons in a heterostructure and lattice strain have been suggested as a means to control the orbital occupation [75]. So far, much of the focus has been on 'conducting versus insulating' behavior. However, a recent discovery has illustrated that such a question does not cover all possibilities. Calculations on VO_2/TiO_2 heterostructures [76], nonpolar and seemingly having only the d^1–d^0 aspect to arouse interest, display a previously unknown electronic structure, consisting of point Fermi surfaces as does graphene, but possessing a highly anisotropic behavior: in the 2D plane the electrons have nearly free character, but in the perpendicular direction the dispersion is massless, like the dispersion (in both directions) in graphene. These 'semi-Dirac' points so far exist only in two-dimensional oxide heterostructures, and their study may rival the activity in graphene. The low energy behavior is distinct [77] not only from graphene but also from another point Fermi surface system, the zero-gap semiconductor. The very different physical structure compared to graphene (robust heterostructure versus a flexible monatomic sheet) will likely lead to very different applications. Fundamental understanding of both polar effects, and the characteristics of dispersion, should be important aspects in future studies.

Finally, another complexity should be noted. In the studies of polar interfaces, correlation effects arising from strong intra-atomic interaction have been shown to lead to very different behavior than arises if such effects are neglected. However, so far such interactions have been treated (nearly always) in a static, mean-field manner. It is one of the fundamental precepts of strongly correlated systems that upon doping (which is very likely to occur at some level, perhaps inadvertently) dynamical processes come into play and determine many of the properties of doped correlated insulators. Including such dynamical effects, and especially doing so self-consistently, will be an important part of the next generation of theoretical modeling of oxide heterostructures.

Acknowledgments

We acknowledge useful discussions with A Brinkman, R Claessen, H Y Hwang, M Huijben, J Mannhart, K Otte, V Pardo, S Sathpathy, N Spaldin, K Terakura and E Tsymbal, and have benefitted from support through the Bavaria-California Technology Center (BaCaTeC), the Kavli Institute for Theoretical Physics, the International Center for Materials Research, US DOE grant DE-FG02-04ER46111 and a grant for computational time at the Leibniz Rechenzentrum.

References

[1] Bozovic I and Eckstein J N 1997 Atomic-level engineering of cuprates and manganites *Appl. Surf. Sci.* **114** 189
[2] Ohtomo A, Muller D A, Grazul J L and Hwang H Y 2002 Artificial charge-modulation in atomic-scale perovskite titanate superlattices *Nature* **419** 378
[3] Ohtomo A and Hwang H Y 2004 A high-mobility electron gas at the $LaAlO_3/SrTiO_3$ heterointerface *Nature* **427** 423
[4] Reyren N *et al* 2007 Superconducting interfaces between insulating oxides *Science* **317** 1196
[5] Brinkman A, Huijben M, van Zalk M, Huijben J, Zeitler U, Maan J C, van der Wiel W G, Rijnders G, Blank D H A and Hilgenkamp H 2007 Magnetic effects at the interface between non-magnetic oxides *Nat. Mater.* **6** 493
[6] Kennedy D 2007 Breakthrough of the year: the runners-up, beyond silicon? *Science* **1318** 1844
[7] Goss Levi B 2007 Interface between insulators may be ferromagnetic and superconducting *Phys. Today* **60** 23
[8] Tasker P W 1979 The stability of ionic crystal surfaces *J. Phys. C: Solid State Phys.* **12** 4977
[9] Noguera C 2000 Polar oxide surfaces *J. Phys.* **12** R367
[10] Goniakowski J, Finocchi F and Noguera C 2008 Polarity of oxide surfaces and nanostructures *Rep. Prog. Phys.* **71** 016501
[11] Nakagawa N, Hwang H Y and Muller D A 2006 Why some interfaces cannot be sharp *Nat. Mater.* **5** 204
[12] Anisimov V I, Solovyev I V, Korotin M A, Czyzyk M T and Sawatzky G A 1993 Density-functional theory and NiO photoemission spectra *Phys. Rev.* B **48** 16929
[13] Blaha P, Schwarz K, Madsen G K H, Kvasnicka D and Luitz J 2001 *WIEN2k* Karlheinz Schwarz, Technical University Wien, Austria (ISBN 3-9501031-1-2)
[14] Perdew J P, Burke K and Ernzerhof M 1996 Generalized gradient approximation made simple *Phys. Rev. Lett.* **77** 3865
[15] Pavarini E, Biermann S, Poteryaev A, Lichtenstein A I, Georges A and Andersen O K 2004 Mott transition and suppression of orbital fluctuations in orthorhombic $3d^1$ perovskites *Phys. Rev. Lett.* **92** 176403

[16] Yoshida C, Tamura H, Yoshida A, Kataoka Y, Fujimaki N and Yokoyami N 1996 Electric field effect in $LaTiO_3/SrTiO_3$ heterostructure *Japan. J. Appl. Phys.* **35** 5691

[17] Ohtomo A, Muller D A, Grazul J L and Hwang H Y 2002 Epitaxial growth and electronic structure of $LaTiO_x$ films *Appl. Phys. Lett.* **80** 3922

[18] Kim K H, Norton D P, Budai J D, Chisholm M F, Sales B C, Christen D K and Cantoni C 2003 Epitaxial structure and transport in $LaTiO_{3+x}$ films on (001) $SrTiO_3$ *Phys. Status Solidi* a **200** 346

[19] Hwang H Y, Ohtomo A, Nakagawa N, Muller D A and Grazul J L 2004 High mobility electrons in $SrTiO_3$ heterostructures *Physica* E **22** 712

[20] Shibuya K, Ohnishi T, Kawasaki M, Koinuma H and Lippmaa M 2004 Growth and structure of wide-gap insulator films on $SrTiO_3$ *Japan. J. Appl. Phys.* **43** L1178

[21] Takizawa M *et al* 2006 Photoemission from buried interfaces in $SrTiO_3/LaTiO_3$ superlattices *Phys. Rev. Lett.* **97** 057601

[22] Okamoto S and Millis A J 2004 Electronic reconstruction at an interface between a Mott insulator and a band insulator *Nature* **428** 630
Okamoto S and Millis A J 2004 *Phys. Rev.* B **70** 075101
Okamoto S and Millis A J 2004 *Phys. Rev.* B **70** 241104
Okamoto S and Millis A J 2005 *Phys. Rev.* B **72** 235108

[23] Kancharla S S and Dagotto E 2006 Metallic interface at the boundary between band and Mott insulators *Phys. Rev.* B **74** 195427

[24] Lee W-C and MacDonald A H 2007 Electronic interface reconstruction at polar–nonpolar Mott-insulator heterojunctions *Phys. Rev.* B **75** 195117

[25] Rüegg A, Pilgram S and Sigrist M 2007 Aspects of metallic low-temperature transport in Mott-insulator/band-insulator superlattices: optical conductivity and thermoelectricity *Phys. Rev.* B **75** 195117
Rüegg A, Pilgram S and Sigrist M 2008 *Phys. Rev.* B **77** 245118

[26] Popovic Z S and Satpathy S 2005 Wedge-shaped potential and airy-function electron localization in oxide superlattices *Phys. Rev. Lett.* **94** 176805

[27] Hamann D R, Muller D A and Hwang H Y 2006 Lattice-polarization effects on electron-gas charge densities in ionic superlattices *Phys. Rev.* B **73** 195403

[28] Pentcheva R and Pickett W E 2007 Correlation-driven charge order at the interface between a Mott and a band insulator *Phys. Rev. Lett.* **99** 016802

[29] Okamoto S, Millis A J and Spaldin N A 2006 Lattice relaxation in oxide heterostructures: $LaTiO_3/SrTiO_3$ superlattices *Phys. Rev. Lett.* **97** 056802

[30] Larson P, Popovic Z S and Satpathy S 2008 Lattice relaxation effects on the interface electron states in the perovskite oxide heterostructures: $LaTiO_3$ monolayer embedded in $SrTiO_3$ *Phys. Rev.* B **77** 245122

[31] Solovyev I, Hamada N and Terakura K 1996 t_{2g} versus all 3d localization in $LaMO_3$ perovskites (M = TiCu): first-principles study *Phys. Rev.* B **53** 7158

[32] Ishida H and Liebsch A 2008 Origin of metallicity of $LaTiO_3/SrTiO_3$ heterostructures *Phys. Rev.* B **77** 115350

[33] Kumagai K, Suzuki T, Taguchi Y, Okada Y, Fujishima Y and Tokura Y 1993 Metal–insulator transition in $La_{1-x}Sr_xTiO_3$ and $Y_{1-x}Ca_xTiO_3$ investigated by specific-heat measurements *Phys. Rev.* B **48** 7636

[34] Tokura Y, Taguchi Y, Okada Y, Fujishima Y, Arima T, Kumagai K and Iye Y 1993 Filling dependence of electronic properties on the verge of metal-Mott-insulator transition in $Sr_{1-x}La_xTiO_3$ *Phys. Rev. Lett.* **70** 2126

[35] Huijben M, Rijnders G, Blank D H A, Bals S, van Aert S, Verbeeck J, van Tendeloo G, Brinkman A and Hilgenkamp H 2006 Electronically coupled complementary interfaces between perovskite band insulators *Nat. Mater.* **5** 556

[36] Herranz G *et al* 2006 High mobility in $LaAlO_3/SrTiO_3$ heterostructures: origin, dimensionality and perspectives *Phys. Rev.* B **73** 064403

[37] Siemons W, Koster G, Yamamoto H, Harrison W A, Lucovsky G, Geballe T H, Blank D H A and Beasley M R 2007 Origin of charge density at $LaAlO_3$ on $SrTiO_3$ heterointerfaces: possibility of intrinsic doping *Phys. Rev. Lett.* **98** 196802

[38] Kalabukhov A, Gunnarsson R, Börjesson J, Olsson E, Claeson T and Winkler D 2007 Effect of oxygen vacancies in the $SrTiO_3$ substrate on the electrical properties of the $LaAlO_3/SrTiO_3$ interface *Phys. Rev.* B **75** 121404(R)

[39] Basletic M, Maurice J-L, Carretero C, Herranz G, Copie O, Bibes M, Jacquet E, Bouzehouane K, Fusil S and Barthelemy A 2008 Mapping the spatial distribution of charge carriers in $LaAlO_3/SrTiO_3$ heterostructures *Nat. Mater.* **7** 621

[40] Rijnders G and Blank D H A 2008 Materials science: build your own superlattice *Nat. Mater.* **7** 270

[41] Gemming S and Seifert G 2006 $SrTiO_3$(001)/$LaAlO_3$(001) multilayers: a density-functional investigation *Acta Mater.* **54** 4299

[42] Pentcheva R and Pickett W E 2006 Charge localization or itineracy at $LaAlO_3/SrTiO_3$ interfaces: hole polarons, oxygen vacancies, and mobile electrons *Phys. Rev.* B **74** 035112

[43] Park M S, Rhim S H and Freeman A J 2006 Charge compensation and mixed valency in $LaAlO_3/SrTiO_3$ heterointerfaces studied by the FLAPW method *Phys. Rev.* B **74** 205416

[44] Popovic Z S, Satpathy S and Martin R M 2008 Origin of the two-dimensional electron gas carrier density at the $LaAlO_3$ on $SrTiO_3$ interface *Phys. Rev. Lett.* **101** 256801

[45] Pentcheva R and Pickett W E 2008 Ionic relaxation contribution to the electronic reconstruction at the *n*-type $LaAlO_3/SrTiO_3$ interface *Phys. Rev.* B **78** 205106

[46] Albina J-M, Mrovec M, Meyer B and Elsässer C 2007 Structure, stability, and electronic properties of $SrTiO_3/LaAlO_3$ and $SrTiO_3/SrRuO_3$ interfaces *Phys. Rev.* B **76** 165103

[47] Maurice J-L *et al* 2007 Charge imbalance at oxide interfaces: how nature deals with it *Mater. Sci. Eng.* B **144** 1

[48] Zhong Z and Kelly P J 2008 Electronic-structure induced reconstruction and magnetic ordering at the $LaAlO_3/SrTiO_3$ interface *Eur. Phys. Lett.* **84** 27001

[49] Janicka K, Velev J P and Tsymbal E Y 2009 Quantum nature of two-dimensional electron gas confinement at $LaAlO_3/SrTiO_3$ interfaces *Phys. Rev. Lett.* **102** 106803

[50] Thiel S, Hammerl G, Schmehl A, Schneider C W and Mannhart J 2006 Tunable quasi-two-dimensional electron gases in oxide heterostructures *Science* **313** 1942

[51] Cen C, Thiel S, Hammerl G, Schneider C W, Andersen K E, Hellberg C S, Mannhart J and Levy J 2008 Nanoscale control of an interfacial metal–insulator transition at room temperature *Nat. Mater.* **7** 298

[52] Pentcheva R and Pickett W E 2009 Avoiding the polarization catastrophe in $LaAlO_3$ overlayers on $SrTiO_3$(001) through polar distortion *Phys. Rev. Lett.* **102** 107602

[53] Salluzzo M *et al* 2009 Orbital reconstruction and the two-dimensional electron gas at the $LaAlO_3/SrTiO_3$ interface *Phys. Rev. Lett.* **102** 166804

[54] Sing M *et al* 2009 Profiling the interface electron gas of $LaAlO_3/SrTiO_3$ heterostructures with hard x-ray photoelectron spectroscopy *Phys. Rev. Lett.* **102** 176805

[55] Son W-J, Cho E, Lee B, Lee J and Han S 2009 Density and spatial distribution of charge carriers in the intrinsic *n*-type $LaAlO_3$–$SrTiO_3$ interface *Phys. Rev.* B **79** 245411

[56] Li Y and Yu J 2009 Polarization screening and induced carrier density at the interface of $LaAlO_3$ overlayer on $SrTiO_3$(001) arXiv:0904.1636 [cond-mat]

[57] Ishibashi S and Terakura K 2008 *J. Phys. Soc. Japan* **77** 104706
[58] Rozzi C A, Varsano C, Marini A, Gross E K U and Rubio A 2006 Exact Coulomb cutoff technique for supercell calculations *Phys. Rev.* B **73** 205119
[59] Chen H, Kolpak A M and Ismail-Beigi S 2009 Fundamental asymmetry in interfacial electronic reconstruction between insulating oxides: an *ab initio* study *Phys. Rev.* B **79** R161402
[60] Schwingenschlögl U and Schuster C 2008 Interface relaxation and electrostatic charge depletion in the oxide heterostructure $LaAlO_3/SrTiO_3$ *Eur. Phys. Lett.* **81** 17007
Schwingenschlögl U and Schuster C 2009 *Eur. Phys. Lett.* **86** 27005
[61] Pavlenko N and Kopp T 2009 Structural relaxation and metal–insulator transition at the interface between $SrTiO_3$ and $LaAlO_3$ arXiv:0901.4610 [cond-mat]
[62] Lee J and Demkov A A 2008 Charge origin and localization at the *n*-type $SrTiO_3/LaAlO_3$ interface *Phys. Rev.* B **78** 193104
[63] Breitschaft M *et al* 2009 Two-dimensional electron liquid state at $LaAlO_3$–$SrTiO_3$ interfaces arXiv:0907.1176 [cond-mat]
[64] Willmott P R *et al* 2007 Structural basis for the conducting interface between $LaAlO_3$ and $SrTiO_3$ *Phys. Rev. Lett.* **99** 155502
[65] Bristowe N C, Artacho E and Littlewood P B 2009 Oxide superlattices with alternating *p* and *n* interfaces *Phys. Rev.* B **80** 045425
[66] Bengtsson L 1999 Dipole correction for surface supercell calculations *Phys. Rev.* B **59** 12301
[67] Natan A, Kronik L and Shapira Y 2006 Computing surface dipoles and potentials of self-assembled monolayers from first principles *Appl. Surf. Sci.* **252** 7608
[68] Bell C, Harashima S, Hikita Y and Hwang H Y 2009 Dominant mobility modulation by the electric field effect at the $LaAlO_3/SrTiO_3$ interface *Appl. Phys. Lett.* **94** 222111
[69] Hotta Y, Wadati H, Fujimori A, Suzaki T and Hwang H Y 2007 Polar discontinuity doping of the $LaVO_3/SrTiO_3$ interface *Phys. Rev. Lett.* **89** 251916
[70] Wadati H *et al* 2008 Hard x-ray photoemission study of $LaAlO_3/LaVO_3$ multilayers *Phys. Rev.* B **77** 045122
[71] Pentcheva R, Huijben M, Otte K, Pickett W E, Kleibeuker J E, Huijben J, Boschker H, Kockmann D, Siemons W, Koster G, Zandvliet H J W, Rijnders G, Blank D H A, Hilgenkamp H and Brinkman A 2009 unpublished
[72] Pentcheva R and Sadat Nabi H 2008 Interface magnetism in $Fe_2O_3/FeTiO_3$-heterostructures *Phys. Rev.* B **89** 251916
[73] Sadat Nabi H and Pentcheva R 2009 Effect of strain on the stability and electronic properties of ferrimagnetic $Fe_{2-x}Ti_xO_3$ heterostructures from correlated band theory *J. Appl. Phys.* **106** 073912
[74] Robinson P, Harrison R J, McEnroe S A and Hargraves R B 2002 Lamellar magnetism in the hematite–ilmenite series as an explanation for strong remanent magnetization *Nature* **418** 517
[75] Chaloupka J and Khaliullin G 2008 Orbital order and possible superconductivity in $LaNiO_3/LaMO_3$ superlattices *Phys. Rev. Lett.* **100** 016404
[76] Pardo V and Pickett W E 2009 Half-metallic semi-Dirac-point generated by quantum confinement in TiO_2/VO_2 nanostructures *Phys. Rev. Lett.* **102** 166803
[77] Banerjee S, Singh R R P, Pardo V and Pickett W E 2009 Tight-binding modeling and low-energy behavior of the semi-Dirac point *Phys. Rev. Lett.* **103** 016402